

PAPER • OPEN ACCESS

An efficient soil penetration strategy for explorative robots inspired by plant root circumnutation movements

To cite this article: Emanuela Del Dottore *et al* 2018 *Bioinspir. Biomim.* **13** 015003

View the [article online](#) for updates and enhancements.

Related content

- [Physical root–soil interactions](#)
Evelyne Kolb, Valérie Legué and Marie-Béatrice Bogeat-Triboulot
- [A novel tracking tool for the analysis of plant-root tip movements](#)
A Russino, A Ascrizzi, L Popova et al.
- [A plant-inspired robot with soft differential bending capabilities](#)
A Sadeghi, A Mondini, E Del Dottore et al.



IOP | ebooks™

Bringing you innovative digital publishing with leading voices to create your essential collection of books in STEM research.

Start exploring the collection - download the first chapter of every title for free.

Bioinspiration & Biomimetics

OPEN ACCESS**PAPER**

An efficient soil penetration strategy for explorative robots inspired by plant root circumnutation movements

RECEIVED
10 May 2017**REVISED**
22 October 2017**ACCEPTED FOR PUBLICATION**
10 November 2017**PUBLISHED**
22 December 2017

Original content from this work may be used under the terms of the [Creative Commons Attribution 3.0 licence](#).

Any further distribution of this work must maintain attribution to the author(s) and the title of the work, journal citation and DOI.

**Emanuela Del Dottore**^{1,2} , **Alessio Mondini**², **Ali Sadeghi**², **Virgilio Mattoli**² and **Barbara Mazzolai**²¹ The BioRobotics Institute, Scuola Superiore Sant'Anna, Pontedera, Italy² Center for Micro-BioRobotics, Istituto Italiano di Tecnologia, Pontedera, ItalyE-mail: emanuela.deldottore@iit.it and barbara.mazzolai@iit.it**Keywords:** bioinspiration, robotics, circumnutations, soil-penetration, plant-inspired-robot

Abstract

This paper presents a comparative analysis in terms of energy required by an artificial probe to penetrate soil implementing two different strategies: a straight penetration movement and a circumnutation, which is an oscillatory movement performed by plant roots. The role of circumnutations in plant roots is still debated. We hypothesized that circumnutation movements can help roots in penetrating soil, and validated our assumption by testing the probe at three distinct soil densities and using various combinations of circumnutation amplitudes and periods for each soil. The comparison was based on the total work done by the system while circumnulating at its tip level with respect to that shown by the same system in straight penetration. The total energy evaluation confirmed an improvement obtained by circumnutations up to 33%. We also proposed a fitting model for our experimental data that was used to estimate energy needed by the probe to penetrate soil at different dimensions and circumnutation amplitudes. Results showed the existence of a trade-off among penetration velocity, circumnutation period, and amplitude toward an energy consumption optimization, expressed by the lead angle of the helical path that should stay in the range between 46° and 65°. Moreover, circumnutations with appropriate amplitude (~10°) and period (~80 s) values were more efficient than straight penetration also at different probe tip dimensions, up to a threshold diameter (from 2 mm to 55 mm). Based on the obtained results, we speculated that circumnutations can represent a strategy used by plant roots to reduce the pressure and energy needed to penetrate soil. The translation of this biological feature in robotic systems will allow improving their energetic efficiency in digging tasks, and thus open new scenarios for use in search and rescue, environmental monitoring, and soil exploration.

1. Introduction

Engineering has looked at plants for making innovations for a long time (e.g. Velcro[®], Lotus Effect[®]). Recently, plants and their roots have been used as a model to design and build robotic technologies, including mechanisms and control solutions (Kim *et al* 2010, Ulrich *et al* 2010, Mazzolai *et al* 2011, Sadeghi *et al* 2014, 2016, Mazzolai 2017). Plants, being sessile organisms, have evolved different strategies of movement, based on an indeterminate growth, and capabilities to adapt their structures to the surrounding environments for anchoring and exploration, providing an important source of inspiration.

Many biological observations, with the appropriate interpretation, can be relevant to engineering,

including robotics. For instance, robots inspired by plant roots could be useful for subsoil exploration, penetration, and monitoring tasks (Sadeghi *et al* 2013). An improvement in performing these tasks can be achieved through the implementation of peculiar movements (i.e. circumnutations) in plant root-like robots. Circumnutations, also known by the general term nutations, are elliptical, circular, or pendulum-like movements performed by the plant organs active in growth (i.e. apical parts of shoot and apical part of roots) (figure 1). This phenomenon is induced by a differential elongation rate at the opposite flanks of the organ (Migliaccio *et al* 2013). Circumnutations have been known since Darwin's studies, but their role in roots is still not completely understood. Among several speculations, it also seems that they have an important role in facilitating soil penetration

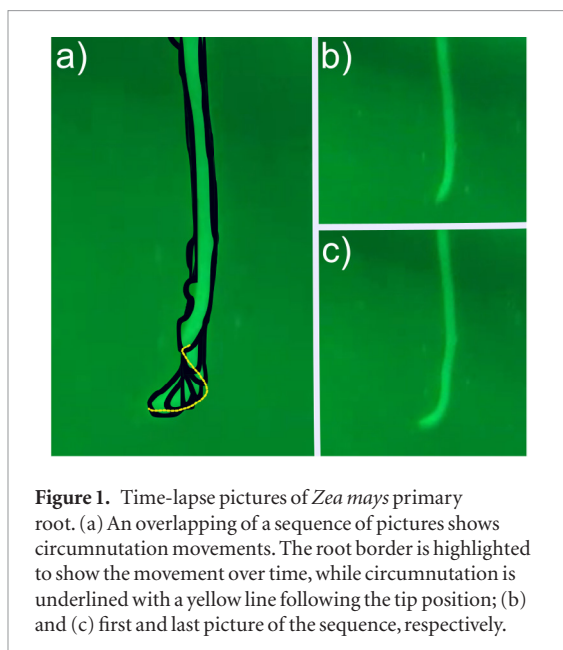


Figure 1. Time-lapse pictures of *Zea mays* primary root. (a) An overlapping of a sequence of pictures shows circumnutation movements. The root border is highlighted to show the movement over time, while circumnutation is underlined with a yellow line following the tip position; (b) and (c) first and last picture of the sequence, respectively.

(Fisher 1964). In *Oryza sativa* L. a better establishment of seeds in paddy fields was observed when root tips rotated at high frequencies performing a spiral growth (Inoue *et al* 1999). Other studies, maybe less obviously connected to circumnutation roles, reported experiments with (i) mechanically stimulated roots, and (ii) unimpeded roots exposed to externally applied ethylene. These studies (Moss *et al* 1988, Sarquis *et al* 1991) revealed similar reactions on root growth: inhibition of longitudinal cell expansion, and promotion of lateral expansion. Ethylene is a phytohormone typically produced by plant roots in specific stress conditions, including mechanical stress (Veen 1982). These observations confirm that plant roots, when mechanically stimulated, produce ethylene that affects cells growth. Later studies demonstrated that ethylene increases root wave amplitude in *Arabidopsis thaliana* (Buer *et al* 2003). Root waving is a phenomenon present in very fine roots—e.g. *Arabidopsis thaliana*—and is ascribed to the interaction among gravity, tactile stimulation, and circumnutations (Mullen *et al* 1998). All the above observations support a correlation between soil mechanical properties and plant root circumnutations: high soil impedance induces stress in plant roots; in stress conditions a root produces ethylene; the increase of ethylene affects its growth and increases wave amplitudes; an alteration of waving can be linked to an alteration of circumnutation movement (Mullen *et al* 1998, Oliva and Dunand 2007).

The role of circumnutations in plant roots can be empirically demonstrated by measuring resistances perceived by roots with and without circumnutations. Various studies have been conducted in the past to estimate the root resistance in different soils by means of penetrometers (for a review on this topic refer to Bengough and Mullins (1990) and Bengough *et al* (2011)). Despite the fact that penetrometers cannot provide the actual resistance experienced by plant roots, and usually give an overestimation (Bengough

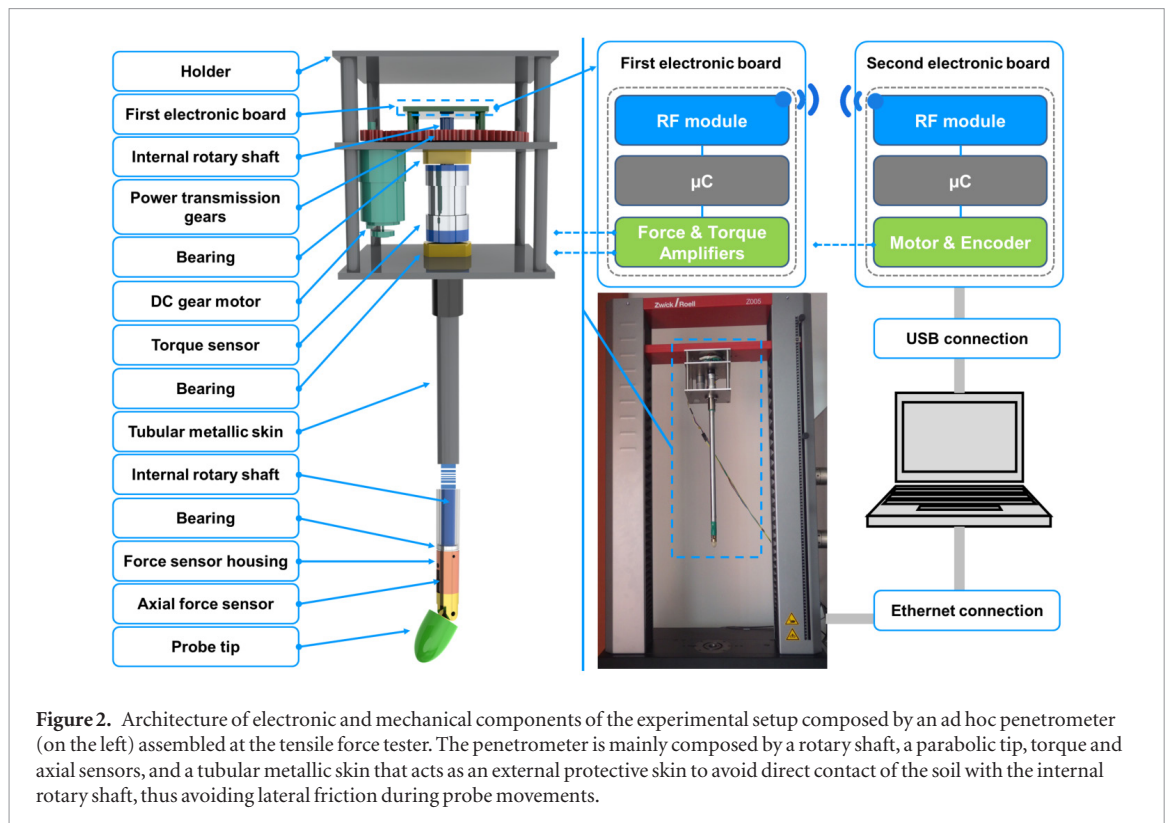
and Mullins 1990), these techniques still represent a valid method for soil penetration and comparative analysis with innovative solutions inspired by plant roots. For instance, Bengough *et al* (1991) proposed a comparison between a straight fixed tip and a straight rotating tip showing a lowering of the total forces perceived by the tester machine when penetrating sandy soil. Similarly, Jung *et al* (2017) analyzed the drag force needed by a conical probe to penetrate an artificial granular soil and glass beads in straight fixed penetration, by rotating the cone while preserving the vertical position. They also obtained a reduction of the forces when tip rotation was applied. However, studies on the effectiveness and efficiency of root circumnutations during soil penetration are still limited. Circumnutation is in fact a more complex movement with respect to a simple rotation in the vertical position of a probe tip, since it involves a misalignment of the tip with respect to the normal axis that is characterized by an amplitude, distance from the nutation axis, and movement frequency. In a previous study, we compared the axial forces necessary for a robotic root pushed from its top to penetrate an artificial soil using straight movements or circumnutations (Del Dottore *et al* 2016). In those experiments we measured up to 80 times less force when circumnutations were used. This demonstrates that such movement is convenient in terms of forces, inducing less stress on the penetration device and reaching higher depth compared to a straight probe movement with the same amount of external applied force. However, in this previous work we neglected the power needed to generate the probe tip's rotary motion.

The present work aims at estimating the efficiency of a root performing circumnutations during soil penetration in terms of energy consumption. We estimated the improvement by means of comparative experiments using a setup purposely developed. With respect to our previous work, we tested the mechanism in a real soil and in a larger (24 cm of diameter) and deeper (30 cm of penetration) environment, scaling down probe and tip dimensions (from 4 to 2 cm) to reduce chamber size effects (Salgado *et al* 1997, Bolton *et al* 1999). We isolated the axial forces applied at the probe tip and torque to evaluate the total energy consumed by the system. We present and discuss the experimental results and the model developed to fit data and predict root behavior at different tip sizes and nutation amplitudes. This work intends to contribute to the scientific discussion on the role of root circumnutations, and lays foundations for designing optimized plant-like robots for drilling and soil exploration.

2. Methods

2.1. Experimental setup

We estimated the energy that a sensorized artificial root requires to penetrate soil with and without circumnutations by performing two series of



experiments. The energy of a straight penetration is given by the perceived axial force, times displacement. In the case of circumnutation, we obtained the total work combining two movements: straight penetration and a rotation. The relative energy was then obtained by simultaneously evaluating the axial force and the torque with the corresponding displacements, through a customized setup (figure 2). The setup included a rigid rotary shaft embedded inside a tubular metallic skin (mimicking the root lateral body) to protect the internal shaft from the lateral friction induced by interaction with the soil along the probe; a parabolic tip (connected to the rotary shaft) to mimic the root tip, with a diameter of 2 cm; an axial force sensor (LSB200—QSH01809—50 kg S-Beam Load Cell from FUTEK Advanced Sensor Technology, Inc.) embedded close to the tip to acquire only the force at tip level; a gear motor used to generate the rotary motion of the shaft; and a torque sensor (TFF350—FSH00645—100 in-lb reaction torque sensor from FUTEK Advanced Sensor Technology, Inc.) directly mounted on top of the rotary shaft to measure the torque applied at the tip level. The setup measured the torque necessary for rotating the tip, and eliminated the effect of any internal disturbing friction or external soil lateral friction from this measure. To accomplish this, the internal frictions on the rotary shaft were minimized by means of rotary bearings between the shaft and tubular skin, while at the same time the tubular skin protected the rotation of shaft from direct contact with soil, and thus eliminated the friction between soil and the rotating shaft. A slider mechanism was used to provide the penetration with constant velocity

(a tensile force tester—Zwick/Roell Z005—was used in this case while the slider moved at a controlled and constant speed).

Figure 2 depicts an overview of the whole setup and its architecture for data acquisition. The axial load cell, torque sensor (mounted on the bottom and top of the shaft), and an electronic board rotated with the shaft to avoid wire twisting during penetration. This board was equipped with two operational amplifiers (LMC6482 from Texas Instruments) to amplify the sensor signals; a microcontroller with a 16 bit analog to digital converter (CY8C3866 from Cypress); a wireless module to transmit data (RFD21733 from RF Digital Corp USA); and a battery for self-powering to avoid any connection to external power supplies. Data sent were collected by a twin wireless module in a second electronic board connected via USB to a PC for data storing. This board was equipped with a 32 bit microcontroller (PIC32MX460 from Microchip) and a motor driver (LV8548MC from ON Semiconductor) to command the shaft rotation by a metal gear motor (50:1 Metal Gearmotor 37D × 70L mm with a 64 CPR Encoder, from Pololu). Motor speed was controlled by implementing a PID control on the microcontroller. The system was managed by a custom user interface developed in VB.NET that permitted us to set the circumnutation period (T) and save the acquired data.

2.2. Experimental protocol and parameters

All penetration experiments were performed in topsoil, which was dried at room temperature for 48 h and then filtered with a 4 × 4 mm net to eliminate big particles and filaments. The experiments were

conducted over 6 weeks in a closed and conditioned environment at 26–28 °C and 63–68% humidity. The soil was inserted into a cylindrical container with a 24 cm diameter and a total height of 52 cm. For each penetration experiment, soil was prepared at three different compactness levels with 0.38 g cm⁻³, 0.40 g cm⁻³, and 0.42 g cm⁻³ densities (ρ). We performed the penetration tests with different circumnutation parameters by placing the tip at (α) 10° and 20° with respect to the vertical axis, and varying a complete rotation period (T) among 30 s, 60 s, 120 s, and 240 s. From our previous experiments (Del Dottore *et al* 2016), we observed that the penetration speed slightly affected the measured forces on the tip. Based on this consideration, we set the probe's velocity (v) at 40 mm min⁻¹, and its penetration at a maximum 30 cm; thus, each experiment lasted 7.5 min. Tests were repeated at least nine times for each experiment (table A1).

2.3. Data acquisition and analysis

Data were acquired every 100 ms (Δt) and saved in csv format with each row containing axial force (F_{V_i}) and torque (τ_i). Axial work (W_V) and rotary work (W_R) were then obtained with the following formulas:

$$W_V = \sum_i (F_{V_i} \cdot v \cdot \Delta t), \quad (1)$$

$$W_R = \sum_i (\tau_i \cdot \omega \cdot \Delta t). \quad (2)$$

Where i identifies the i th row acquired from 0 to 30 cm of penetration, v is the penetration velocity, and $\omega = 2\pi/T$ is the angular velocity. The instantaneous work can be defined as the work for each time step as follows:

$$W_i = (F_{V_i} \cdot v \cdot \Delta t) + (\tau_i \cdot \omega \cdot \Delta t). \quad (3)$$

The total work is simply obtained by

$$W_{\text{Tot}} = W_V + W_R. \quad (4)$$

Normality of data (W_{Tot}) was tested with the Shapiro–Wilk test (appendix), considering separately each set of samples grouped on the basis of combinations of period, amplitude, and soil density (table A1). Since the groups were not normally distributed, Levene's test (appendix) was then used to test the equality of variances (tables A2–A4). Considering the presence of non-normal distributions and unequal variances, Friedman's test (appendix) was used on the averaged energy for each group to compare the effects of period, amplitude, and density factors (tables A5 and A6).

3. Results

3.1. Experimental results

Huang *et al* (2004) presented a model for a conical penetrometer that showed how the resistance at the cone in homogeneous soil stabilized after 0.1–0.3 m of penetration. The point of stabilization changed

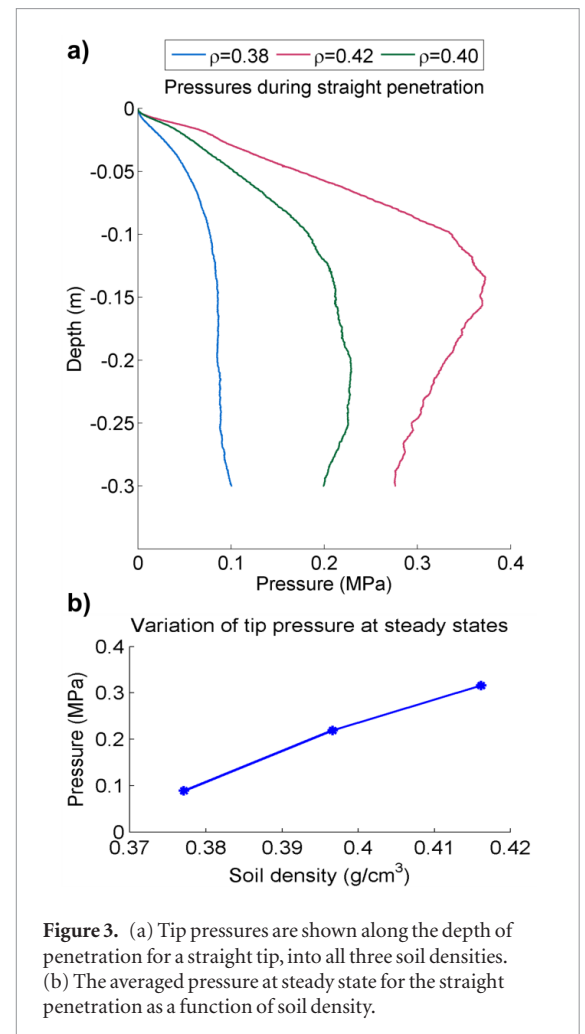


Figure 3. (a) Tip pressures are shown along the depth of penetration for a straight tip, into all three soil densities. (b) The averaged pressure at steady state for the straight penetration as a function of soil density.

according to different pressure and soil internal friction factors. The same behavior has been observed in penetrometer tests conducted over five different laboratories (Bolton *et al* 1999). This steady state can also be identified with the pressures obtained in our straight penetration experiments (figure 3(a)), where, after 0.15–0.25 m traveled, the force needed by the tip for pushing remains approximately constant; consequently, the instantaneous energy, obtained as in (3), reaches a maximum value (table 1). Figure 3(b) shows the almost linear increase of tip pressures obtained from our experiments as a function of soil density, at steady state. Similarly, Huang *et al* (2004) obtained a linear increasing cone resistance at steady state as a function of soil pressure.

Table 2 shows an example of exclusively axial forces (coaxial with the shaft) perceived by the tip in straight penetration and with circumnutations, both taken as averaged forces at steady state (after half of the total experiment time—from 0.15 m); the percentage of improvement is from 66 to 78% in the three soils.

However, in the presence of circumnutations, forces involved in the rotary movement should be considered, and consequently the energy is affected. Figure 4 shows an example of instantaneous energy consumed by the system along the entire penetration with circumnutations, together with straight penetra-

Table 1. Mean, minimum, and maximum values of the instantaneous axial energies (J) after half of the vertical trajectory (from 0.15 to 0.3 m) in each soil for the straight penetration.

	Axial energy (J)		
	$\rho = 0.38 \text{ g cm}^{-3}$	$\rho = 0.40 \text{ g cm}^{-3}$	$\rho = 0.42 \text{ g cm}^{-3}$
Mean	0.0019	0.0053	0.0068
Min	0.0018	0.0048	0.0060
Max	0.0021	0.0056	0.0079

Table 2. Averaged axial forces obtained in straight penetration and with circumnutations at 10° amplitude and 60 s period. The improvement is obtained as a percentage of the difference among the two forces over straight penetration.

	$\rho = 0.38 \text{ g cm}^{-3}$	$\rho = 0.40 \text{ g cm}^{-3}$	$\rho = 0.42 \text{ g cm}^{-3}$
Straight penetration (N)	27.90	61.92	99.23
Circumnutations (N)	6.03	20.06	33.65
Improvement (%)	78	68	66

tion energy, in the three soils at different densities. With circumnutations, we can observe that after reaching a depth of ~ 0.15 m the energy stops increasing and tends to oscillate around a stable value. This kind of behavior confirms the existence of a limit depth below which soil resistance converges to an asymptote (Tardos *et al* 1998, Guillard *et al* 2013, 2015).

The total energy obtained for each experimental group for the whole displacement of 30 cm is presented in figure 5(a). Analyzing the work done by the system, the energy consumed increases with soil density. Although we varied the tip angle and nutation period, we obtained an improvement for most of the combinations (figure 5(b)), up to 33.12% at 10° on the lighter soil with respect to the straight penetration (table 3).

Energy is then presented as a function of the nutation period (figure 6). In figure 6 the energy of straight penetration is used for comparison (black, solid and dashed lines). The same conclusions can be reached from the curves and statistical analysis with a 95% confidence interval: all period variation affect the energy among different amplitudes in the same way ($P = 0.1447$ in $\rho = 0.38 \text{ g cm}^{-3}$ and $\rho = 0.40 \text{ g cm}^{-3}$, $P = 0.1870$ in $\rho = 0.42 \text{ g cm}^{-3}$). Meanwhile, amplitudes provide ($P = 0.0455$) slightly different effects among periods on $\rho = 0.38 \text{ g cm}^{-3}$ and $\rho = 0.42 \text{ g cm}^{-3}$, but a greater effect ($P = 0.3173$) on $\rho = 0.40 \text{ g cm}^{-3}$. Furthermore, the effect of different soil density is extremely significant ($P = 0.0001$). On each curve it is possible to observe a minimum located below each black line in a range from 60 s to 120 s, where lower energy is obtained.

3.2. Fitting model

To better describe the behavior emerging from our results, we analyzed the system's motion and the forces

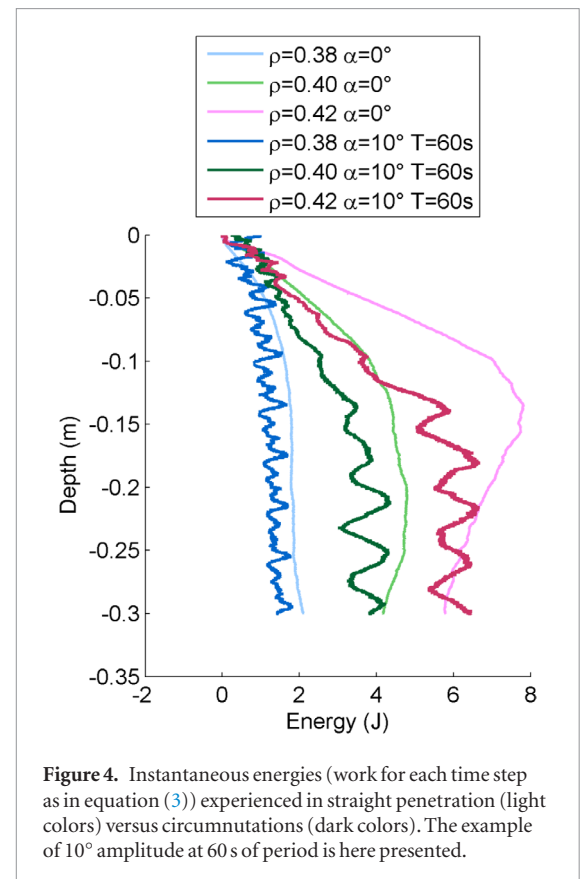


Figure 4. Instantaneous energies (work for each time step as in equation (3)) experienced in straight penetration (light colors) versus circumnutations (dark colors). The example of 10° amplitude at 60 s of period is here presented.

involved at steady state, where those forces became stable and reached the maximum value. The tip, while moving in soil with fine granularity, performs a circular movement with angular velocity ω and a linear movement coaxial to the shaft with velocity v . The combination of these two movements provides a helical path (figure 7(a)). For the formed helix, it is possible to define pitch $P_0 = v \cdot T$ and lead angle $\varepsilon = a \tan(P_0/\pi d)$. The probe tip has approximately a parabolic shape with diameter d_n and length l .

The problem of defining the total pushing force during the movement is equal to defining the resistance force acting only on the probe tip. Different from in viscous fluids, in granular soil there are complex combinations of force chains among particles that rearrange and propagate anisotropically and inhomogeneously when an object moves in it (Albert *et al* 1999, Takada and Hayakawa 2016). This condition makes the problem of modelling an object moving into real soil still an open question. However, some work on this has been done; for instance, the independence between penetration velocity and the force needed by an object to move into a granular medium has been demonstrated when velocity is low (Albert *et al* 1999, 2001, Guillard *et al* 2015), as well as the independence from depth when a limit depth is reached (Tardos *et al* 1998, Guillard *et al* 2013, 2015), thus allowing approximation of the pressure in the soil below such limit depth with $\sim \rho g a$, where ρ is the bulk density, g is the gravity acceleration, and a is a coefficient that should take into account soil parameters, e.g. internal friction angle, compressibility and water content. As a matter

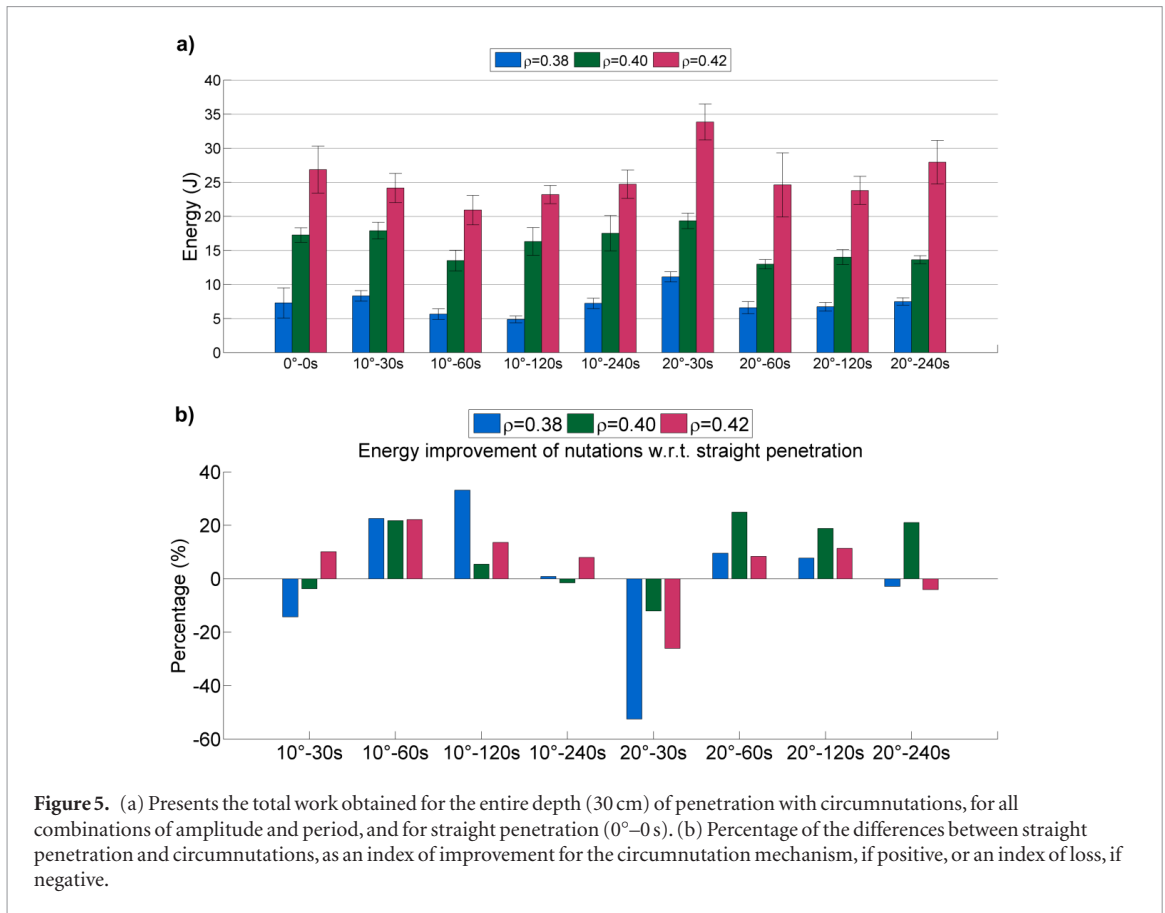


Figure 5. (a) Presents the total work obtained for the entire depth (30 cm) of penetration with circumnutations, for all combinations of amplitude and period, and for straight penetration (0°–0 s). (b) Percentage of the differences between straight penetration and circumnutations, as an index of improvement for the circumnutation mechanism, if positive, or an index of loss, if negative.

Table 3. Maximum value of improvement on the energies obtained with circumnutations with respect to the straight penetration; second and third columns indicate respectively the angle and period with which the improvement is obtained.

	Improvement (%)	α (°)	T (s)
$\rho = 0.38 \text{ g cm}^{-3}$	33.12	10	120
$\rho = 0.40 \text{ g cm}^{-3}$	24.88	20	60
$\rho = 0.42 \text{ g cm}^{-3}$	22.13	10	60

of fact, bulk density alone cannot express soil compactness and pressure among different types of soil (clay, sand, loam, etc). Having a relatively low penetration velocity in our experimental conditions, we can assume independence from v , which is an assumption particularly true for plants; since we are considering only the part of the experiment in steady state condition, we can also assume independence from depth. With these assumptions and previous considerations, during lateral movement the tip needs to exert a force proportional to the pressure exercised by the soil on the lateral area of the tip:

$$F_r = C_r \rho g \mu_r \tag{5}$$

Here, μ_r is a dimensionless coefficient, and C_r (m^3) is defined as follows:

$$C_r = \iint x \cdot f(x, y) \cdot dx \cdot dy, \tag{6}$$

where $f(x, y)$ is a logical function that defines the inclusion of a point in the area of the parabolic tip

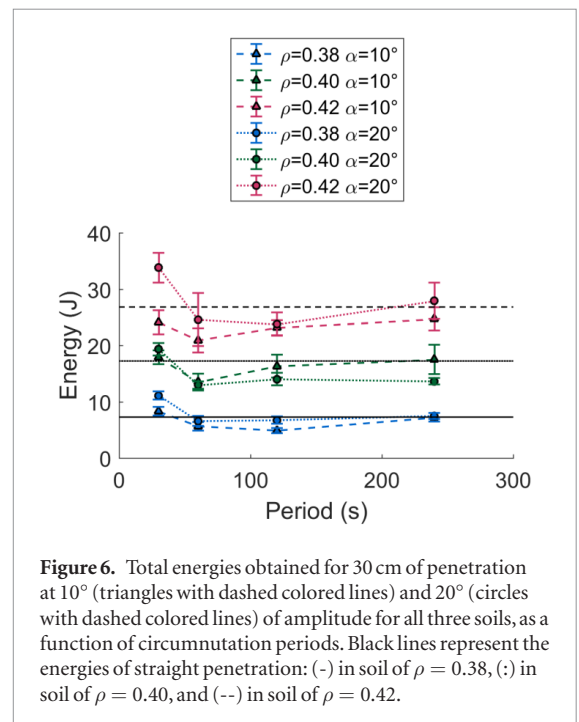


Figure 6. Total energies obtained for 30 cm of penetration at 10° (triangles with dashed colored lines) and 20° (circles with dashed colored lines) of amplitude for all three soils, as a function of circumnutation periods. Black lines represent the energies of straight penetration: (-) in soil of $\rho = 0.38$, (·) in soil of $\rho = 0.40$, and (- -) in soil of $\rho = 0.42$.

exposed to lateral soil interaction ($f(x, y) = 1$ if the point (x, y) is into the grey area in figure 7(b); $f(x, y) = 0$ otherwise), and x is the radius for each column of the tip. The integral

$$A_r = \iint f(x, y) \cdot dx \cdot dy \tag{7}$$

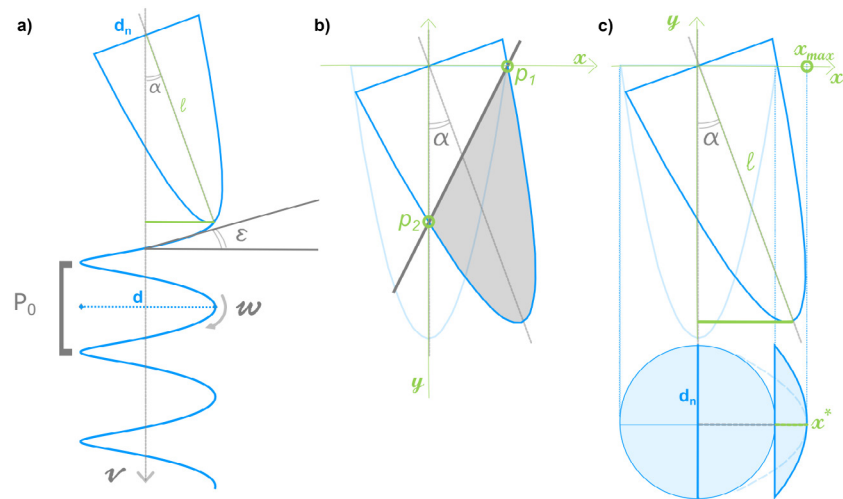


Figure 7. Geometrical representation of tip: (a) helical path traced by a tilted tip, with main parameters; (b) the surface involved in rotary motion is highlighted in gray, and is represented by the portion of the parabola under the line between p_1 and p_2 , where p_1 is the point of intersection with the parabola and y -axis, and p_2 is the point of intersection between the parabola and x -axis; (c) the surface involved in axial penetration is the bottom projection of the tip (in light blue).

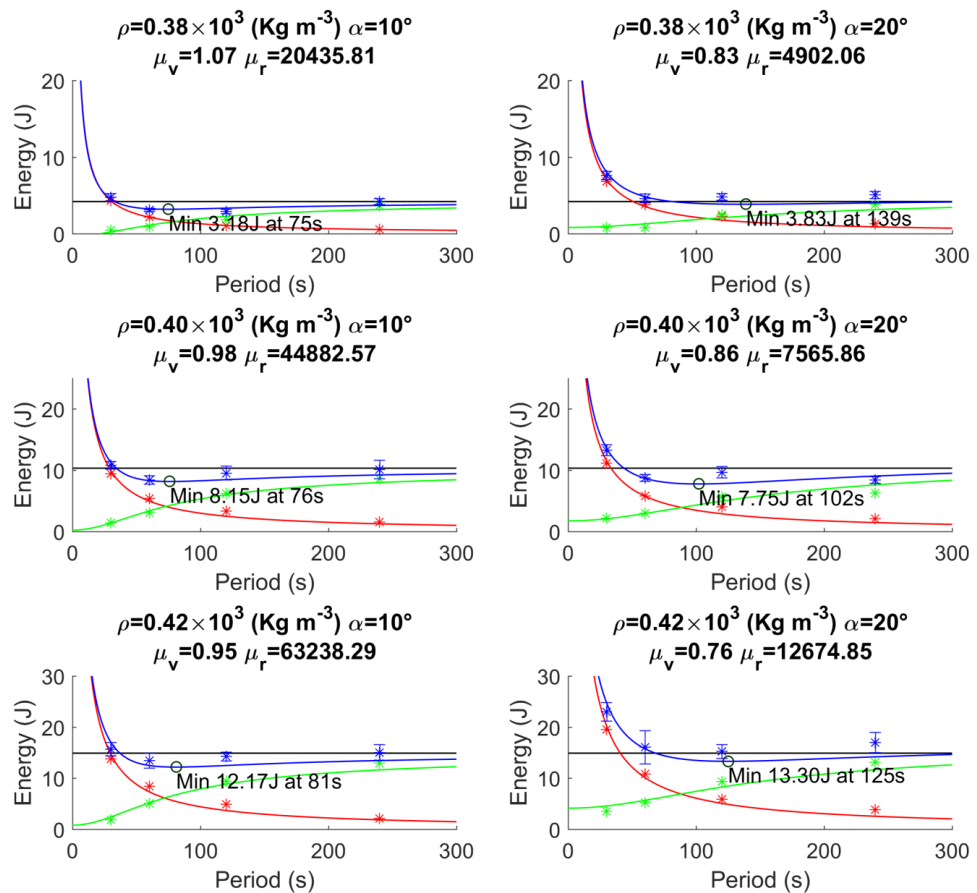


Figure 8. Fitting curves of energy at 10° and 20° in all three soils. Total fitting curves (blue lines) are obtained by summing up fitting of vertical energies (green lines) with fitting of rotational energies (red lines). Stars with error bars represent mean values of experimental data with standard deviations obtained at four periods of nutation (30, 60, 120, and 240 s). Black lines are the energies found with straight penetration in each soil. Energies correspond to the average among all repetitions for each combination, considering only the total work (as in (4)) for the displacement in the steady state condition (from 0.15 to 0.3 m). The minimum point is indicated with a dark circle on each curve, along with the corresponding energy and period. Points were obtained by imposing a lower bound equal to 0 on μ_v and μ_r .

is the cross sectional area in a plane of the tip exposed to lateral soil interaction. The rotary work can be obtained by the following:

$$W_R = F_r \cdot \Delta s_R, \quad (8)$$

where Δs_R is the distance traveled by the tip along the helical path

$$\Delta s_R = \frac{C_r}{A_r} \omega \cdot T_{\text{exp}}, \quad (9)$$

where T_{exp} is the time spent in the vertical distance traveled (Δs_v).

For the axial movement, the force needed for pushing the tip (F_v) can be approximated with a function proportional to the area (A_v) directly affected by the axial pressure (P_v) (Whiteley et al 1981):

$$F_v = A_v P_v (1 - \mu_v \cos \varepsilon). \quad (10)$$

In (10), P_v is the pressure obtained from the energy of the straight penetration experiments. Nevertheless, taking into account that nutations affect soil compaction and particle rearrangement, we corrected this pressure with a factor depending on nutation parameters, that are expressed in equation (10) by ε , and are weighted with a dimensionless coefficient (μ_v): the high frequency of nutation movement can lighten the pressure under the penetrometer ($\varepsilon \rightarrow \pi/2$ and $\cos \varepsilon \rightarrow 1$), while with a low frequency, soil pressure tends to reflect the pressure of straight penetration ($\varepsilon \rightarrow 0$ and $\cos \varepsilon \rightarrow 0$).

The area (A_v) of the bottom-down projection of the tip (figure 7(c)) is obtained by

$$A_v = \left(\frac{d_n}{2}\right)^2 \pi + \frac{2}{3} d_n x^*, \quad (11)$$

where d_n is the tip diameter, and x^* is obtained by subtracting the shaft radius from the maximal x point of the parabolic shape. The axial work can then be obtained by

$$W_V = F_v \cdot \Delta s_v. \quad (12)$$

The vertical and rotational work found experimentally are fitted separately and then summed together. The total work is indeed given by the sum of (8) and (12). Unknown parameters of the model are μ_v and μ_r , which are obtained through data fitting.

The total work fitted at steady state is presented in figure 8. Each curve has a minimum under which the energy remains lower with respect to the energy found in straight penetration. On average, the point of minimum energy is located at ~ 77 s with $\alpha = 10^\circ$, and ~ 122 s with $\alpha = 20^\circ$. For the corresponding amplitude these periods bring an energetic advantage with respect to the straight penetration in every soil. An asymptotic behavior is present at the extremities:

$$\begin{cases} \lim_{T \rightarrow 0} W_{\text{Tot}}^T = +\infty \\ \lim_{T \rightarrow \infty} W_{\text{Tot}}^T = Y \end{cases},$$

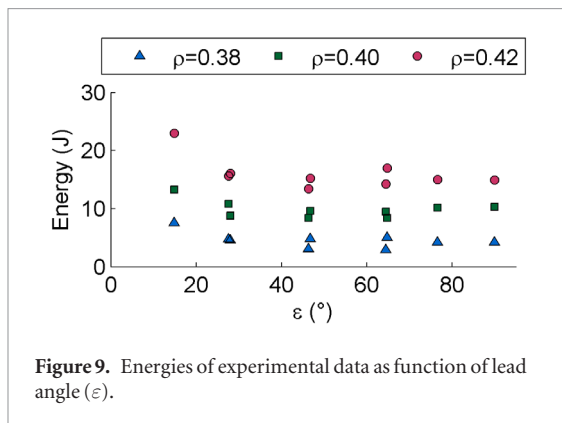
where Y is a finite value that represents the energy associated with a straight penetration performed with the tip bent.

Considering the parameters obtained by the fitting, we can observe fluctuations of μ_v around a relatively stable value: 1 with $\alpha = 10^\circ$, and ~ 0.82 with $\alpha = 20^\circ$; μ_r has instead an almost linear increase over soil density (with linear equation $\mu_r = 1.1 \cdot 10^3 \rho - 3.9 \cdot 10^5$ for $\alpha = 10^\circ$, and $\mu_r = 2 \cdot 10^2 \rho - 6.9 \cdot 10^4$ for $\alpha = 20^\circ$). Both decrease with increasing amplitudes in each soil, suggesting that not only the soil compactness changes with different densities, but also that circumnutation amplitudes can affect soil compactness: a bigger amplitude means a greater area exposed to soil interaction, thus resulting in dislocation of a greater amount of soil, and therefore less pressure (lower μ_v and μ_r) compared to a smaller amplitude (higher μ_v and μ_r).

4. Discussions

4.1. Setup and model considerations

This paper presented an experimental method and a data fitting model aimed at improving the scientific knowledge on the role of plant root circumnutations during soil penetration. Limitations of the experimental approach are the number of repetitions that can be performed, and the repeatability of the experimental conditions over a long period of time, since environmental conditions, such as temperature and humidity, can influence soil characteristics. We have confined this risk by performing experiments in an air conditioned room and within a relatively short period of time (6 weeks). Another limitation is probably induced by the protocol used for soil compaction, i.e. rotating the container, tapping on the side, and pressing from the top the soil. This procedure shows at the highest density ($\rho = 0.42$) some pressure inhomogeneity from one layer to another that is caused by an apparent decrease of soil pressure in straight penetration (figure 3, from 0.15 to 0.25 m). However, reaching a steady state in soil pressure has been demonstrated with lower densities, and the literature confirms the presence of a steady state penetrating granular soil (Tardos et al 1998, Guillard et al 2013, 2015), thus suggesting that going deeper or with a more uniform density, it could be possible to reach pressure stability also with $\rho = 0.42$. Our experiments aimed at comparing penetration tests performed with and without circumnutations, and varying nutation amplitude and period. Moreover, we proposed a fitting model based on the analysis of the forces required at steady state by the probe in axial configuration and in rotary movement. Since in our experiments only the soil density was known, all the other soil-related characteristics (i.e. soil internal friction and cohesion, particles interaction, and soil-system interaction properties) were embedded in two unknown coefficients, μ_r and μ_v , which were then



found by our fitting function. Despite its simplicity, the model demonstrates its efficacy by fitting the energy values found at different experimental conditions (i.e. soil density, and nutation amplitude and period). Variation of μ_v and μ_r parameters also let us appreciate the variability of soil compactness that increases with soil density (increasing μ_v and μ_r) and decreases with circumnutation amplitude (decreasing μ_v and μ_r), suggesting the reduction in soil pressure induced by circumnutations. We estimated the range of angular velocities to which the system optimizes energy to move in three different soil densities at a fixed penetration velocity. As demonstrated by our results, with a circumnutation period less than 30 s the system significantly increases the rotary work with consequent high energy consumption; on the other hand, for a circumnutation period greater than 120 s, the system does not obtain any particular advantage in using circumnutations during penetration. This observation suggests that a balance between penetration and angular velocities is required for energy optimization. Since the relation between penetration and angular velocities is included in the lead angle (ϵ) value, we can consider energy as a function of ϵ (figure 9) and find minimum energy values with ϵ between 46° and 65° . With ϵ being a function of nutation period T and amplitude α , if we fix a period of 77 s, we can find that circumnutation amplitudes between 6° and 13° can provide an optimal energy value.

Although we developed the setup to purposively reduce errors in the experimental phase, penetration tests in confined environments are influenced by side effects on soil resistance values. A complete absence of side effects is obtained with a minimum ratio between the container and tip diameter of 40 (Bolton and Gui 1993). In our experiments, we obtained a ratio of 12 for a probe tip with a 2 cm diameter. This ratio was mainly imposed by the dimension of a commercially available load cell that fits in our design of the container, which has to be kept maneuverable. Despite these constraints, the obtained results demonstrate the absence of side effects because of the presence of the steady state. Besides, the comparative analysis between the two different penetration strategies with the same probe

further reduces the importance of these side effects, since we are not interested in defining an absolute cone resistance value.

Additionally, we disregarded experiments using tips with different diameters in the same container deliberately to avoid the occurrence of side effects. Such effects can only be nullified by preserving a minimum ratio between container and tip diameter as a function of soil relative density (Salgado *et al* 1997, Bolton *et al* 1999). We estimated the influence of diameter variation on root behavior using the developed model function.

Figure 10 shows an example (in soil $\rho = 0.40$) of predictions obtained with different nutation amplitudes assuming the behavior of μ_v and μ_r to be linear. Function evaluations are performed by scaling up or down the entire tip size (d_n and l), fixing period T to 77 s, utilizing a constant ratio between pitch and tip diameter ($v \cdot T/d_n = 2.6$), having a constant number of circles performed ($T_{\text{exp}}/T = 2.9$), and by obtaining μ_v and μ_r through linear fitting of the corresponding values obtained at 10° and 20° for the three soil densities. As previously stated for the straight penetration, based on Whiteley *et al* (1981), we assumed that the force exercised on the tip of different dimensions is linearly dependent on the tip diameter (equation (10) with $\epsilon = 0$). Results show that energies increase with tip diameter. All selected amplitudes are convenient for diameters comparable to those of plant roots (figure 10(a)) but the positive improvement of circumnutations is preserved only until a threshold diameter that varies with the amplitude is reached. The existence of an optimal amplitude that minimizes energy consumption is evident in table 3, which shows the greatest improvement for each soil with an amplitude of 10° or 20° . The curves in figure 10(c) also confirm this trend where the lowest energy for a tip diameter greater than 3 cm was obtained with the amplitude of 11° , which brings an advantage for diameters less than 6 cm.

4.2. Circumnutations in plant roots

The obtained results lead us to assume that circumnutations may represent a key mechanism to generate cavity expansion and crack propagation in the soil plastic zone, i.e. the cylindrical zone surrounding the penetration cavity where stresses are sufficient to cause failure (Salgado *et al* 1997).

Study of the circumnutation role in plant roots required simplification of several conditions with respect to natural behavior. *In primis*, we used a faster penetration velocity compared to plant growth; besides, our system is forced to penetrate coaxially with the shaft while plant movements are influenced by environmental stimuli such as nutrients, water, or gravity, and also takes advantage of soil cracks. Moreover, root interaction with soil is completely different, in terms of friction, particle interactions, and the mechanism of penetration, compared with the effects generated by a mechanical device that moves in the same

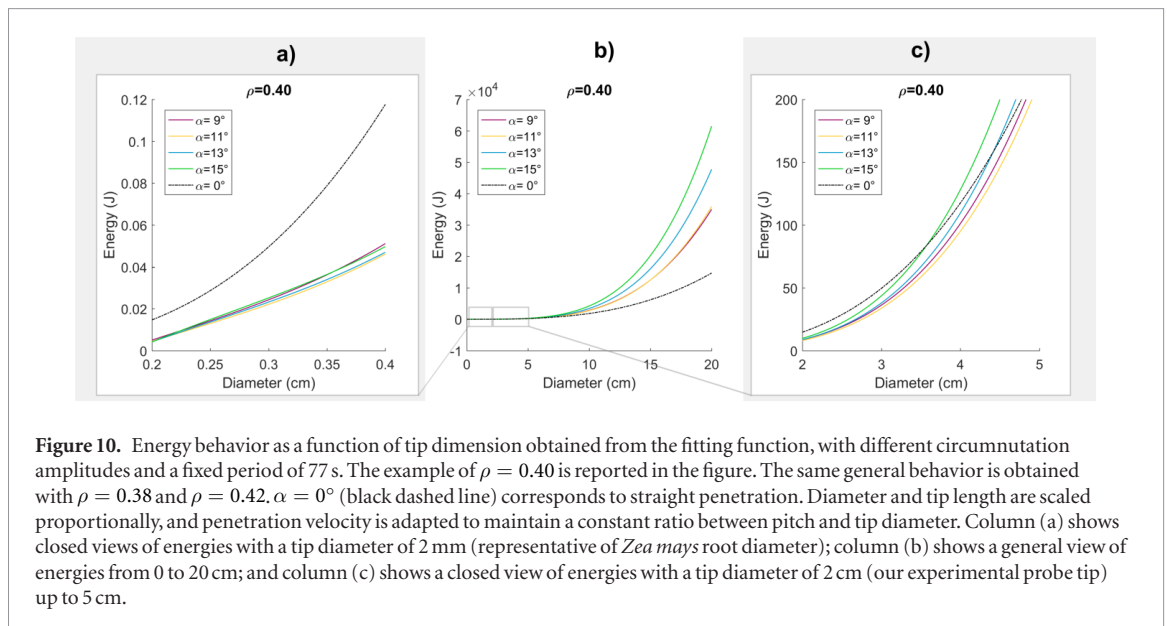


Figure 10. Energy behavior as a function of tip dimension obtained from the fitting function, with different circumnutation amplitudes and a fixed period of 77 s. The example of $\rho = 0.40$ is reported in the figure. The same general behavior is obtained with $\rho = 0.38$ and $\rho = 0.42$. $\alpha = 0^\circ$ (black dashed line) corresponds to straight penetration. Diameter and tip length are scaled proportionally, and penetration velocity is adapted to maintain a constant ratio between pitch and tip diameter. Column (a) shows closed views of energies with a tip diameter of 2 mm (representative of *Zea mays* root diameter); column (b) shows a general view of energies from 0 to 20 cm; and column (c) shows a closed view of energies with a tip diameter of 2 cm (our experimental probe tip) up to 5 cm.

medium. Plant roots move in soil through cell division and elongation phenomena at their tip, and thus, they reduce stress and friction at this level. Through these simplifications, growing and elongation effects were reproduced by positioning the load cell close to the tip and by employing a protective skin, thus allowing the artificial system to only perceive forces and torque acting at the tip level. By doing so, a comparison between the natural and artificial mechanisms—in terms of efficiency of straight versus circumnutation-based soil penetration—is still possible and even sustainable.

From our previous biological experiments (Del Dottore et al 2016) we observed circumnutations in *Zea mays* primary roots with a period between 60–80 min and amplitudes with a radius of 0.2 mm on average. Assuming that circumnutations occur in the central elongation zone (Okada and Shimura 1990), which is the root region with the highest cell elongation rate, and placed in maize at about 4 mm from the tip (Ishikawa and Evans 1993), a radius of 0.2 mm corresponds to $\sim 3^\circ$ of nutation amplitude. Considering a growing rate for *Zea mays* of 1.59 mm h^{-1} (Del Dottore et al 2016), ε is $\sim 52^\circ$, a value perfectly in the range of optimal ε found with our previously presented analysis.

4.3. Circumnutations for robotic roots

Soil is still an environment little explored in robotics, especially for objective difficulties in penetration. However, autonomous devices able to move in subsoil are of interest in either terrestrial and space applications, for exploration (mapping of an area) or source localization (water or other relevant substances), in environmental monitoring, rescue, and other tasks. The presented results confirm the idea that circumnutation is an advantageous mechanism in terms of energy needed to penetrate; indeed, our tests demonstrated a reduction up

to 33% of work done by the probe while using circumnutations with respect to straight penetration. Even just considering the axial forces at the tip level, we obtained significant results: 78% less force with circumnutations in the case of a 10° amplitude and 60 s period. We also observed that the energetic advantage can be preserved through a variety of different tip sizes by tuning circumnutation parameters (figure 10). Clearly, an actual evaluation of energetic performance will depend on the efficiency of the actuators in use. An accurate energetic analysis should be done to evaluate, per each actuation system, the feasibility of the nutation mechanism and the effective power saving. All presented results and considerations suggest that robots, as well as autonomous penetrometer devices, can increase their performance by stress reduction and save energy by implementing this natural movement. Taking inspiration from plant roots we can effectively extract new technologies and strategies for subsoil exploration. Future works will be focused on integrating growing abilities (Laschi et al 2016, Sadeghi et al 2017) together with circumnutations in root-inspired robots, exploiting and maximizing the advantages of both strategies.

Appendix. Statistical analysis

The total energies (W_{Tot}) obtained for the whole displacement of 30 cm are tested to verify their significance. As first test, we should evaluate the normality of data. Since not all groups have the same cardinality, the Shapiro–Wilk test (Royston 1982, 1992, 1993a, 1993b, 1995) is used. Results are reported in table A1.

Next, we should evaluate the heteroscedasticity (equality of variances) among multiple combinations of the groups (tables A2–A4). Since not all the groups

Table A1. Groups of experiments with their cardinality, averaged total energy, and the results of the Shapiro–Wilk test implemented in MATLAB^a.

	α	T	$ G_i $	Energy (J)	P	Normality ($P > 0.05$)
$\rho = 0.38$						
G_1	0	0	13	7.2751	0.003	No
G_2	10	30	10	8.3128	0.707	Yes
G_3	10	60	10	5.6340	0.001	No
G_4	10	120	10	4.8655	0.768	Yes
G_5	10	240	9	7.2141	0.006	No
G_6	20	30	10	11.0950	0.516	Yes
G_7	20	60	10	6.5822	0.226	Yes
G_8	20	120	10	6.7120	0.360	Yes
G_9	20	240	10	7.4839	0.558	Yes
$\rho = 0.40$						
G_{10}	0	0	9	17.2446	0.365	Yes
G_{11}	10	30	10	17.8857	0.688	Yes
G_{12}	10	60	10	13.4937	0.625	Yes
G_{13}	10	120	10	16.3028	0.909	Yes
G_{14}	10	240	10	17.5061	0.808	Yes
G_{15}	20	30	10	19.3244	0.623	Yes
G_{16}	20	60	10	12.9544	0.723	Yes
G_{17}	20	120	10	14.0042	0.788	Yes
G_{18}	20	240	10	13.6220	0.840	Yes
$\rho = 0.42$						
G_{19}	0	0	10	26.8451	0.641	Yes
G_{20}	10	30	10	24.1332	0.115	Yes
G_{21}	10	60	10	20.9037	0.930	Yes
G_{22}	10	120	10	23.1881	0.639	Yes
G_{23}	10	240	10	24.7144	0.153	Yes
G_{24}	20	30	10	33.8340	0.129	Yes
G_{25}	20	60	10	24.6010	0.055	Yes
G_{26}	20	120	10	23.7815	0.544	Yes
G_{27}	20	240	10	27.9363	0.756	Yes

^a <https://it.mathworks.com/matlabcentral/fileexchange/13964-shapiro-wilk-and-shapiro-francia-normality-tests/content/swtest.m>

Table A3. Comparison of variances obtained from groups with different circumnutation periods but in the same soil and with the same amplitude.

				P	Equality
G_2	G_3	G_4	G_5	0.639	Yes
G_6	G_7	G_8	G_9	0.724	Yes
G_{11}	G_{12}	G_{13}	G_{14}	0.234	Yes
G_{15}	G_{16}	G_{17}	G_{18}	0.151	Yes
G_{20}	G_{21}	G_{22}	G_{23}	0.417	Yes
G_{24}	G_{25}	G_{26}	G_{27}	0.004	No

were normally distributed, Levene’s test is used for heteroscedasticity (Leven 1960). The test is performed with the function *vartestn* in MATLAB with the Levene option test type. Equality of variances is accepted if the P value is greater than 0.05.

Table A2. Variances of straight penetration (G_1, G_{10} , and G_{19}) are compared with the variances of nutating groups for each soil separately.

	P	Equality
G_1		
G_2	0.001	No
G_3	0.001	No
G_4	0.000	No
G_5	0.001	No
G_6	0.001	No
G_7	0.002	No
G_8	0.000	No
G_9	0.000	No
G_{10}		
G_{11}	0.644	Yes
G_{12}	0.469	Yes
G_{13}	0.086	Yes
G_{14}	0.075	Yes
G_{15}	0.946	Yes
G_{16}	0.125	Yes
G_{17}	0.941	Yes
G_{18}	0.053	Yes
G_{19}		
G_{20}	0.181	Yes
G_{21}	0.154	Yes
G_{22}	0.017	Yes
G_{23}	0.120	Yes
G_{24}	0.424	Yes
G_{25}	0.071	Yes
G_{26}	0.155	Yes
G_{27}	0.699	Yes

Table A4. Comparison of variances obtained at different amplitudes but with the same period and soil.

		P	Equality
G_2	G_6	0.732	Yes
G_3	G_7	0.399	Yes
G_4	G_8	0.353	Yes
G_5	G_9	0.523	Yes
G_{11}	G_{15}	0.624	Yes
G_{12}	G_{16}	0.071	Yes
G_{13}	G_{17}	0.084	Yes
G_{14}	G_{18}	0.010	No
G_{20}	G_{24}	0.538	Yes
G_{21}	G_{25}	0.001	No
G_{22}	G_{26}	0.064	Yes
G_{23}	G_{27}	0.278	Yes

Due to the presence of non-normal and non-heteroscedastic groups, Friedman’s test is used to test the effects of period, amplitude, and density factors (tables A5 and A6). The test is performed in MATLAB with the designated function *friedman*.

Table A5. Effects of amplitude and period compared on each single soil. For a P value less than 0.05 the null hypothesis, that the effects for the specific factor are the same among samples, is rejected.

				P
G_2	G_3	G_4	G_5	
G_6	G_7	G_8	G_9	
Effect of amplitude				0.0455
Effect of period				0.1447
G_{11}	G_{12}	G_{13}	G_{14}	
G_{15}	G_{16}	G_{17}	G_{18}	
Effect of amplitude				0.3173
Effect of period				0.1447
G_{20}	G_{21}	G_{22}	G_{23}	
G_{24}	G_{25}	G_{26}	G_{27}	
Effect of amplitude				0.0455
Effect of period				0.1870

Table A6. The effect of soil density tested among all groups for each soil.

			P
G_1	G_{10}	G_{19}	
G_2	G_{11}	G_{20}	
G_3	G_{12}	G_{21}	
G_4	G_{13}	G_{22}	
G_5	G_{14}	G_{23}	
G_6	G_{15}	G_{24}	
G_7	G_{16}	G_{25}	
G_8	G_{17}	G_{26}	
G_9	G_{18}	G_{27}	
Effect of density			0.0001

ORCID iDs

Emanuela Del Dottore  <https://orcid.org/0000-0001-6874-1970>

References

- Albert R, Pfeifer M A, Barabási A L and Schiffer P 1999 Slow drag in a granular medium *Phys. Rev. Lett.* **82** 205
- Albert I, Sample J G, Morss A J, Rajagopalan S, Barabási A L and Schiffer P 2001 Granular drag on a discrete object: shape effects on jamming *Phys. Rev. E* **64** 061303
- Bengough A G and Mullins C E 1990 Mechanical impedance to root growth: a review of experimental techniques and root growth responses *Eur. J. Soil Sci.* **41** 341–58
- Bengough A G, Mullins C E, Wilson G and Wallace J 1991 The design, construction and use of a rotating-tip penetrometer *J. Agric. Eng. Res.* **48** 223–7
- Bengough A G, McKenzie B M, Hallett P D and Valentine T A 2011 Root elongation, water stress, and mechanical impedance: a review of limiting stresses and beneficial root tip traits *J. Exp. Bot.* **62** 59–68
- Bolton M D and Gui M W 1993 *The Study of Relative Density and Boundary Effects for Cone Penetration Tests in Centrifuge* (Cambridge: Cambridge University Press)
- Bolton M D, Gui M W, Garnier J, Corte J F, Bagge G, Laue J and Renzi R 1999 Centrifuge cone penetration tests in sand *Géotechnique* **49** 543–52
- Buer C S, Wasteney G O and Masle J 2003 Ethylene modulates root-wave responses in Arabidopsis *Plant Physiol.* **132** 1085–96
- Del Dottore E, Mondini A, Sadeghi A, Mattoli V and Mazzolai B 2016 Circumnutations as a penetration strategy in a plant-root-inspired robot *2016 IEEE Int. Conf. on Robotics and Automation (ICRA)* (IEEE) pp 4722–8
- Fisher J E 1964 Evidence of circumnutational growth movements of rhizomes of *Poa pratensis* L. that aid in soil penetration *Canad. J. Bot.* **42** 293–9
- Guillard F, Forterre Y and Pouliquen O 2013 Depth-independent drag force induced by stirring in granular media *Phys. Rev. Lett.* **110** 138303
- Guillard F, Forterre Y and Pouliquen O 2015 Origin of a depth-independent drag force induced by stirring in granular media *Phys. Rev. E* **91** 022201
- Huang W, Sheng D, Sloan S W and Yu H S 2004 Finite element analysis of cone penetration in cohesionless soil *Comput. Geotech.* **31** 517–28
- Inoue N, Arase T, Hagiwara M, Amano T, Hayashi T and Ikeda R 1999 Ecological significance of root tip rotation for seedling establishment of *Oryza sativa* L. *Ecol. Res.* **14** 31–8
- Ishikawa H and Evans M L 1993 The role of the distal elongation zone in the response of maize roots to auxin and gravity *Plant Physiol.* **102** 1203–10
- Jung W, Choi S M, Kim W and Kim H Y 2017 Reduction of granular drag inspired by self-burrowing rotary seeds. *Phys. Fluids* **29** 041702
- Kim S W, Koh J S, Cho M and Cho K J 2010 Towards a bio-mimetic flytrap robot based on a snap-through mechanism *2010 3rd IEEE RAS and EMBS Int. Conf. on Biomedical Robotics and Biomechanics (BioRob)* pp 534–9
- Laschi C, Mazzolai B and Cianchetti M 2016 Soft robotics: technologies and systems pushing the boundaries of robot abilities *Sci. Robot.* **1** eaah3690
- Leven H 1960 Robust test for equality of variances *Contributions to Probability and Statistics: Essays in Honor of Harold Hotelling* ed I Olkin (Palo Alto, CA: Stanford University Press) pp 278–92
- Mazzolai B, Mondini A, Corradi P, Laschi C, Mattoli V, Sinibaldi E and Dario P 2011 A miniaturized mechatronic system inspired by plant roots for soil exploration *IEEE/ASME Trans. Mechatronics* **16** 201–12
- Mazzolai B 2017 Plant-inspired growing robots *Soft Robotics: Trends, Applications and Challenges* (Berlin: Springer) pp 57–63
- Migliaccio F, Tassone P and Fortunati A 2013 Circumnutation as an autonomous root movement in plants *Am. J. Bot.* **100** 4–13
- Moss G I, Hall K C and Jackson M B 1988 Ethylene and the responses of roots of maize (*Zea mays* L.) to physical impedance *New Phytol.* **109** 303–11
- Mullen J L, Turk E, Johnson K, Wolverton C, Ishikawa H, Simmons C, Söll D and Evans M L 1998 Root-growth behavior of the Arabidopsis mutant rgr1: roles of gravitropism and circumnutation in the waving/coiling phenomenon *Plant Physiol.* **118** 1139–45
- Okada K and Shimura Y 1990 Reversible root tip rotation in Arabidopsis seedlings induced by obstacle-touching stimulus *Science* **250** 274
- Oliva M and Dunand C 2007 Waving and skewing: how gravity and the surface of growth media affect root development in Arabidopsis *New Phytol.* **176** 37–43
- Royston J P 1982 An extension of Shapiro and Wilk's W test for normality to large samples *Appl. Stat.* **1** 115–24
- Royston P 1993a A pocket-calculator algorithm for the shapiro-francia test for non-normality: an application to medicine *Stat. Med.* **12** 181–4
- Royston P 1993b A toolkit for testing for non-normality in complete and censored samples *Statistician* **1** 37–43
- Royston P 1995 Remark AS R94: a remark on algorithm AS 181: the W -test for normality *J. R. Stat. Soc. C* **44** 547–51
- Sadeghi A, Tonazzini A, Popova L and Mazzolai B 2013 Robotic mechanism for soil penetration inspired by plant root *2013*

- IEEE Int. Conf. on Robotics and Automation (ICRA)* (IEEE) pp 3457–62
- Sadeghi A, Tonazzini A, Popova L and Mazzolai B 2014 A novel growing device inspired by plant root soil penetration behaviors *PLoS One* **9** e90139
- Sadeghi A, Mondini A, Del Dottore E, Mattoli V, Beccai L, Taccola S, Lucarotti C, Totaro M and Mazzolai B 2016 A plant-inspired robot with soft differential bending capabilities *Bioinspiration Biomimetics* **12** 015001
- Sadeghi A, Mondini A and Mazzolai B 2017 Towards self-growing soft robots inspired by plant roots and based on additive manufacturing technologies *SoRo* **4** 211–23
- Salgado R, Mitchell J K and Jamiolkowski M 1997 Cavity expansion and penetration resistance in sand *J. Geotech. Geoenviron. Eng.* **123** 344–54
- Sarquis J I, Jordan W R and Morgan P W 1991 Ethylene evolution from maize (*Zea mays* L.) seedling roots and shoots in response to mechanical impedance *Plant Physiol.* **96** 1171–7
- Takada S and Hayakawa H 2016 Drag law of two-dimensional granular fluids *J. Eng. Mech.* **143** C4016004
- Tardos G I, Khan M I and Schaeffer D G 1998 Forces on a slowly rotating, rough cylinder in a Couette device containing a dry, frictional powder *Phys. Fluids* **10** 335–41
- Ulrich E R, Humbert J S and Pines D J 2010 Pitch and heave control of robotic samara micro air vehicles *J. Aircr.* **47** 1290–9
- Veen B W 1982 The influence of mechanical impedance on the growth of maize roots *Plant Soil* **66** 101–9
- Whiteley G M, Utomo W H and Dexter A R 1981 A comparison of penetrometer pressures and the pressures exerted by roots *Plant Soil* **61** 351–64